Damage Mechanism of Control Springs in Modular Expansion Joints of Long-Span Bridges

Tong Guo, M.ASCE[1]; Lingyu Huang[2]; Jie Liu[3]; and Yi Zou[4]

Abstract: Premature damage in modular expansion joints, especially in control springs, has been observed in several long-span bridges, which calls for an in-depth study on the damage mechanism. In this study, relative movements of lamellae at different locations of the expansion joints were measured in bridge service condition. It is found that the movements of lamellae were nonuniform, and lamellae near the approximately fixed end of the expansion joint showed much larger relative movements than center lamellae. As a result, control springs underneath these lamellae presented more severe damage than the others. To simulate the behavior of the expansion joint, a finite-element (FE) model was developed, through which the vertical load bearing, horizontal slide friction, and self-equivalence of lamella spacing were modeled, and static and dynamic FE analyses were conducted to obtain the responses of control springs at different locations. Finally, four control springs were tested in a laboratory, in which there was no damage under monotonic loading with shear deformation of 80 mm, whereas under high-cycle loading, two damage patterns were observed, i.e., falling off of the metal head and shear cracking in the rubber cylinder. As cyclic displacement amplitudes increased, the lives of control springs decreased significantly. **DOI: 10.1061/(ASCE)BE.1943-5592.0001255.** *© 2018 American Society of Civil Engineers.*

Author keywords: Modular expansion joints; Long-span bridge; Control spring; Field measurement; Finite-element (FE) simulation; Laboratory test.

Introduction

Expansion joints are commonly used on bridges to accommodate movements resulting from thermal deformations, traffic vibrations, and natural hazards. Effective functioning of expansion joints is not only required for smooth traffic but also for ensuring bridge performance in extreme events, such as earthquakes and hurricanes (Chouw and Hao 2008). Therefore, it is important that these joints work effectively and durably under a range of loading types and conditions. However, expansion joints are dynamically loaded by truck wheels crossing the joint, and their premature damage has been widely noted, including anchorage pullout, bearing failure, debris accumulation, joint overextension, and so forth (Baker Engineering and Energy 2006). For long-span suspension and cable-stayed bridges, finger joints (often with longitudinal movements of 100–1,000 mm) and modular joints (with the movement capacity of over 1,000 mm) are usually used. For modular joints that are investigated in this study, the movements of lamella beams can either be regulated through the rigid system, including the swivel-joist or scissor control systems (Roeder 1998), or through the elastic systems that use elastomeric springs to restore the elements of the joint to their original positions though tensile/compressive or shear deformations of the springs (Guo et al. 2016). Because long-span bridges are relatively flexible and sensitive to vibration (Feng and Feng 2016), the expansion joints have complex stress and movement situations and are prone to damage, even in service condition (Zhao and Roddis 2000; Sun and Zhang 2016; Guo et al. 2015, 2016; Cao et al. 2011). Repair or replacement of expansion joints is often costly and results in undesirable traffic interruption.

During the last decades, there has been extensive analytical and experimental research on expansion joints in which emphasis was placed on the vertical static and dynamic responses of joints under traffic loading as well as their structural integrity based on fatigue, strength, and service requirements (Roeder 1998; Dexter et al. 2001; Crocetti and Edlund 2003; McCarthy et al. 2014; Ding et al. 2016). Based on these studies, guidance to improve the design of, manufacture of, and installation of expansion joints has been given in design and testing specifications (AASHTO 2012). However, fewer studies have focused on the longitudinal behavior of expansion joints under service loads when the joints have complex horizontal working mechanisms, including slide friction, self-equivalence of lamella spacing, movement restraints, and inherent damping and stiffness (McCarthy et al. 2014). Among the limited investigations on horizontal performance of expansion joints, Guo et al. (2016) conducted field monitoring and time and frequency domain analyses of displacements at girder ends. They found that the small but rapid girder displacements due to vehicle/wind loads contributed mostly to the large cumulative displacements, resulting in accelerated damage of control springs and wear of friction materials as well as bridge bearings. In their study, global responses of the joints rather than local response of individual components were investigated; however, field investigation showed that the damage was more severe at certain locations.

In this study, to obtain more in-depth knowledge of the damage mechanism of individual components of expansion joints, especially

[1]Professor, Key Laboratory of Concrete and Prestressed Concrete Structures Ministry of Education, Southeast Univ., Nanjing 210096, P.R. China (corresponding author). E-mail: guotong@seu.edu.cn

[2]Postgraduate Researcher, School of Civil Engineering, Southeast Univ., Nanjing 210096, P.R. China. E-mail: hly0119@hotmail.com

[3]Ph.D. Candidate, School of Civil Engineering, Southeast Univ., Nanjing 210096, P.R. China. E-mail: jieliu@seu.edu.cn

[4]Postgraduate Researcher, School of Civil Engineering, Southeast Univ., Nanjing 210096, P.R. China. E-mail: zy492694251@yahoo.com

Note. This manuscript was submitted on September 22, 2017; approved on January 15, 2018; published online on April 24, 2018. Discussion period open until September 24, 2018; separate discussions must be submitted for individual papers. This paper is part of the ***Journal of Bridge Engineering***, © ASCE, ISSN 1084-0702.

for the damage of control springs, field displacement measurements were conducted at different locations of the expansion joints of a long-span suspension bridge in normal service condition. A finite-element (FE) model was developed to investigate the static and dynamic movements of lamellae. Laboratory tests on four control springs were further performed to verify the conclusions of field measurements and FE analyses, and to preliminarily quantify the lives of control springs under various displacement amplitudes.

Field Displacement Measurements

Bridge Description

The field measurements were conducted on the Runyang Suspension Bridge (RSB), as shown in Fig. 1(a). The RSB has a main span of 1,490 m and was the longest suspension bridge in China and the third longest in the world when it was open to traffic in 2005. The bridge adopted aerodynamically shaped closed steel box-girders in its main span and prestressed concrete (PSC) box-girders in its side spans. In between the steel and PSC box-girders are four modular expansion joints installed for two-way traffic, each with a movement capacity of 2,160 mm, which were largest in the world at that time. As shown in Fig. 1(b), the lamellae rest on and slide along support bars through the upper slide springs, and they are connected by stirrups through which the support bars pass. Between stirrups and support bars are precompressed elastomeric components, i.e., the lower sliding springs in Fig. 1(b). The support bars span between support bar boxes in the deck structures at each side of the movement gap (MAGEBA 2008). The movements of the lamellae relative to each other and along the support bars are regulated through shear deformation of control springs (also known as polymer equidistant devices).

Although the expansion joints were elaborately designed and manufactured, premature damage was observed soon after the bridge was open to traffic. Most often, damage in control springs was seen, as shown in the soffit of the expansion joint in Fig. 1(c), in which springs near the edge beams on the PSC box-girder side seemed more vulnerable. Except for the small thermal deformation of the PSC box-girder, this end of the expansion joint can be regarded as approximately fixed. Typical damage patterns of springs include falling off of the metal head and wear of rubber, as shown in Fig. 2(a). Residual deformations in stirrups were also observed, as shown in Fig. 2(b), which might be due to increased friction force after the severe wear of sliding materials. Also, some movement restraint belts, which allow the lamellae to have a maximum relative movement of 80 mm, were also damaged. Thus, the replacement of damaged belts and installation of more belts were conducted, as shown in Fig. 1(c). Every year, 100–200 control springs were replaced and other expansion joint components repaired, all of which were costly.

Field Measurements and Discussion

To reveal the damage mechanism of expansion joints in service condition, field displacement measurements were conducted on the north end, upstream side of the RSB on March 10, 2017. As shown in Fig. 3(a), one measure point (i.e., P1) was installed underneath the northernmost stirrup below the emergency lane to measure the relative movements between the stirrup of edge lamella and the PSC girder. P3 was installed to measure the relative movements between stirrups of the first and third lamellae, and P5 was installed to measure the relative movements between stirrups of the two center lamellae. Similarly, three measure points (i.e., P2, P4, P6) were installed underneath the stirrups between the center and slow lanes. Displacements at the six measure points were measured using the rod gauge with a measure range of ±10 cm, as shown in Fig. 3(b). Although these points were installed to measure the horizontal

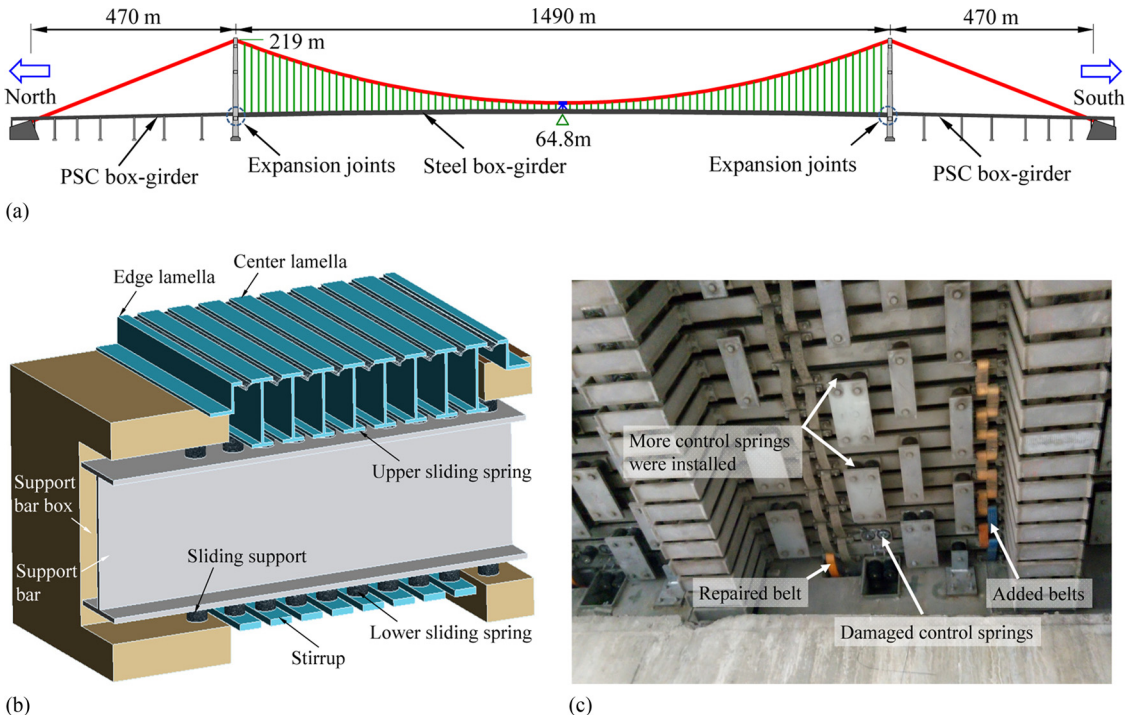

Fig. 1. RSB and its expansion joints: (a) bridge profile; (b) configuration of a modular expansion joint; (c) soffit of the expansion joint (taken in March 2017)

Fig. 2. Field-observed damage: (a) damage in the control spring; (b) residual deformation of stirrups

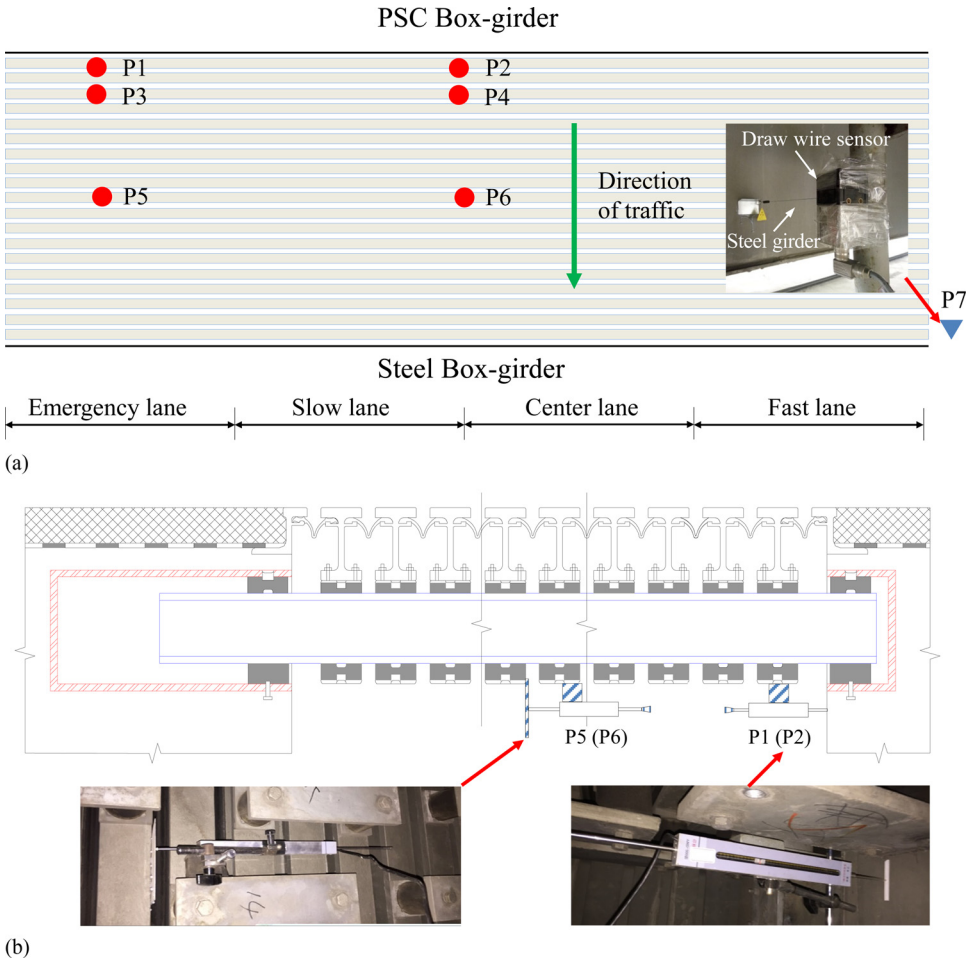

Fig. 3. Layout of measure points: (a) plan view; (b) profile

displacements, they were probably influenced by vertical or torsional deformations of expansion joints as heavy trucks passed. In this regard, Points P1, P3, and P5 underneath the emergency lane were more reliable than Points P2, P4, and P6 because generally no trucks directly passed through the emergency lane during the measurement. Another measure point P7 was installed at the bridge pylon to measure the movements of the steel box-girder by using the draw wire sensor, as shown in Fig. 3(a). All the displacement data were collected at a rate of 20 Hz.

Fig. 4 shows the girder movement time history of Point P7, and the original data show an S shape with a large number of burrs, which was the result of the coupled action of daily temperature fluctuation and vehicle/wind loads. To obtain the traffic/wind-induced movements, a Butterworth filter (Butterworth 1930) was used (Guo et al. 2015). As shown in Fig. 4, it is believed that the low-pass data (with frequencies lower than 5×10^{-5} Hz) were mainly thermal movements, whereas the high-pass data (with frequencies higher than 5×10^{-5} Hz) were mostly induced by vehicle/wind loads. According to Fig. 4, the vehicle/wind load-induced movements are basically within ± 150 mm, and these movements should be properly accommodated through the lamellae of the expansion joints.

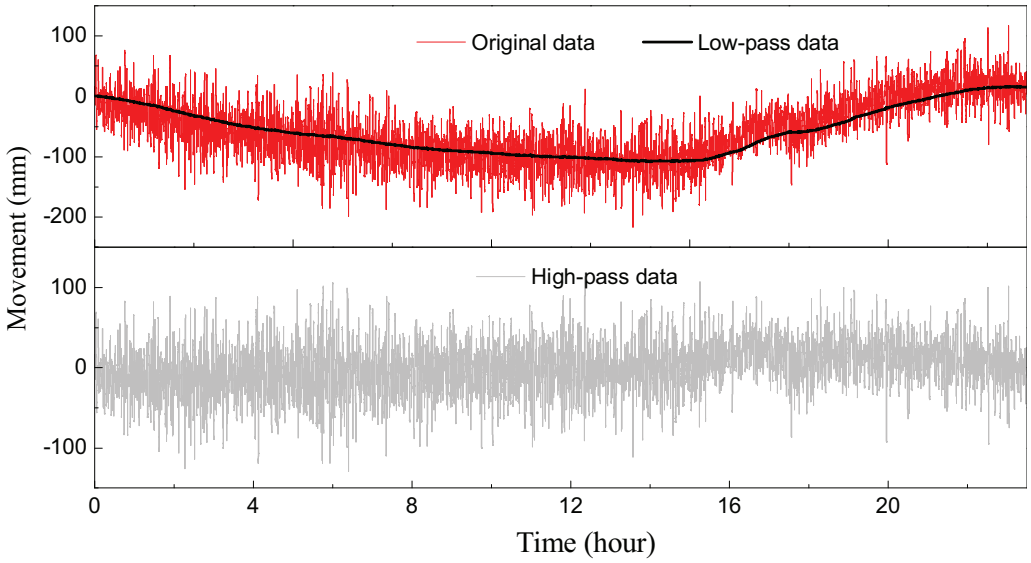

Fig. 4. Daily movement time histories of measure point P7

Fig. 5 further shows the movement time histories of measure points P1–P6, respectively, in which the data are the high-pass type and only results for 30 minutes are shown for clarity. There were larger movements at P1 and P2 than at the other points, and more small burrs could be observed in Fig. 5(b), which was due to the local vibration of lamellae under passing tire loads. When a heavy truck passed through the expansion joint, there was about a 5-cm vertical local deformation in lamellae, resulting in some influence on the measurement of horizontal movements. Generally, the movements at P1 and P2 were synchronous, indicating that the lamella had certain horizontal stiffness. For Points P5 and P6, the movements became much smaller. The peak movements of Points P1–P6 were 30.1, 28.54, 23.0, 18.6, 15.3, and 5.8 mm, respectively. Therefore, movements of these lamellae were nonuniform. Such a characteristic is inconsistent with the field-observed damage distribution. During the measurement, significant noises could be heard as the expansion joints were moving, especially underneath the center lane near measure point P2, indicating that some damage might exist in this region.

FE Simulation and Movement Analysis

FE Modeling

As shown in Fig. 6, the expansion joint is a complicated mechanical system that has a double-load transfer mechanism. Vertically, the wheel load is directly undertaken by the lamellae and then transferred to the support bar through the upper sliding springs; the support bar then transfers the vertical load to the sliding supports in support bar boxes. Horizontally, when there is a movement Δ at the girder end (i.e., thermal movements or vehicle-induced girder movements), a series of friction forces f_i would be generated on the interfaces between the upper and lower sliding springs and the support bar, as shown in Fig. 6(b).

In this study, because the horizontal load is the main reason for the field-observed damage, a FE model was developed using the software *ANSYS 10* (2005), as shown in Fig. 7, to simulate the horizontal behavior of expansion joint. The lamellae, support bars, and stirrups were all modeled using the three-dimensional beam element (i.e., the BEAM188 element); the upper and lower sliding springs and control springs were modeled using the spring-damper element (i.e., the COMBIN14 element); and the friction between sliding springs and support bars was simulated using the contact element (i.e., the CONTA175 element). All the structural components were modeled according to their real dimensions, whereas considering the height of support bars, BEAM188 elements assigned with large stiffnesses (i.e., rigid beams) were used, connecting the support bar and the upper and lower sliding springs, as shown in Fig. 7. The elastic modulus, Poisson's ratio, and density of steel were 2.05×10^5 MPa, 0.25, and 7.8×10^3 kg/m^3, respectively. According to the information provided by the manufacturer based on laboratory tests, the vertical stiffnesses of the upper and lower springs were 550 kN/mm and 6,000 N/mm, respectively, and the friction coefficient of the sliding material was 0.007. The shear stiffness of the control spring was about 100 N/mm, and the cross-sectional area was 4,776mm^2. To facilitate the FE modeling, the control springs were modeled in tension/compression, and the longitudinal stiffness of the element was determined according to the shear stiffness of the control springs.

Static Analysis of Movements in Expansion Joints

First, the responses of the expansion joint under static girder movement (e.g., thermal deformation of steel girders) are investigated. As shown in Fig. 8(a), the lamellae of the expansion joint are labeled from left to right as L_0, L_1, …, L_{27}, respectively; accordingly, the spacing between lamellae are labeled as δ_1, δ_2,…δ_{27}, respectively. Presuming that there was a girder movement of 100 mm at L_0, resulting in a compressive movement of the expansion joint, while lamella L_{27} was fixed, the movements of the lamellae and stresses of the control springs were calculated using the developed FE model, as shown in Fig. 8. Fig. 8(b) shows that from L_0 to L_{27} the movements of lamellae decrease gradually, whereas the relative sliding distance between the sliding springs and support bar increase. Also, the spacing between lamellae is nonuniform. The original spacing of 40 mm, and a rapid reduction in lamella spacing, are observed near the edge lamellae at the fixed end (i.e., L_{27}). Also, the number of springs in δ_1 and δ_{27} (i.e., 10) are only half of those in other spacings (i.e., 20). These two factors result in significantly larger shear stress in control springs in δ_{27}, which is the main reason for the field-observed damage. As shown in Fig. 8(a), from L_0 to L_{27} the total shear force of

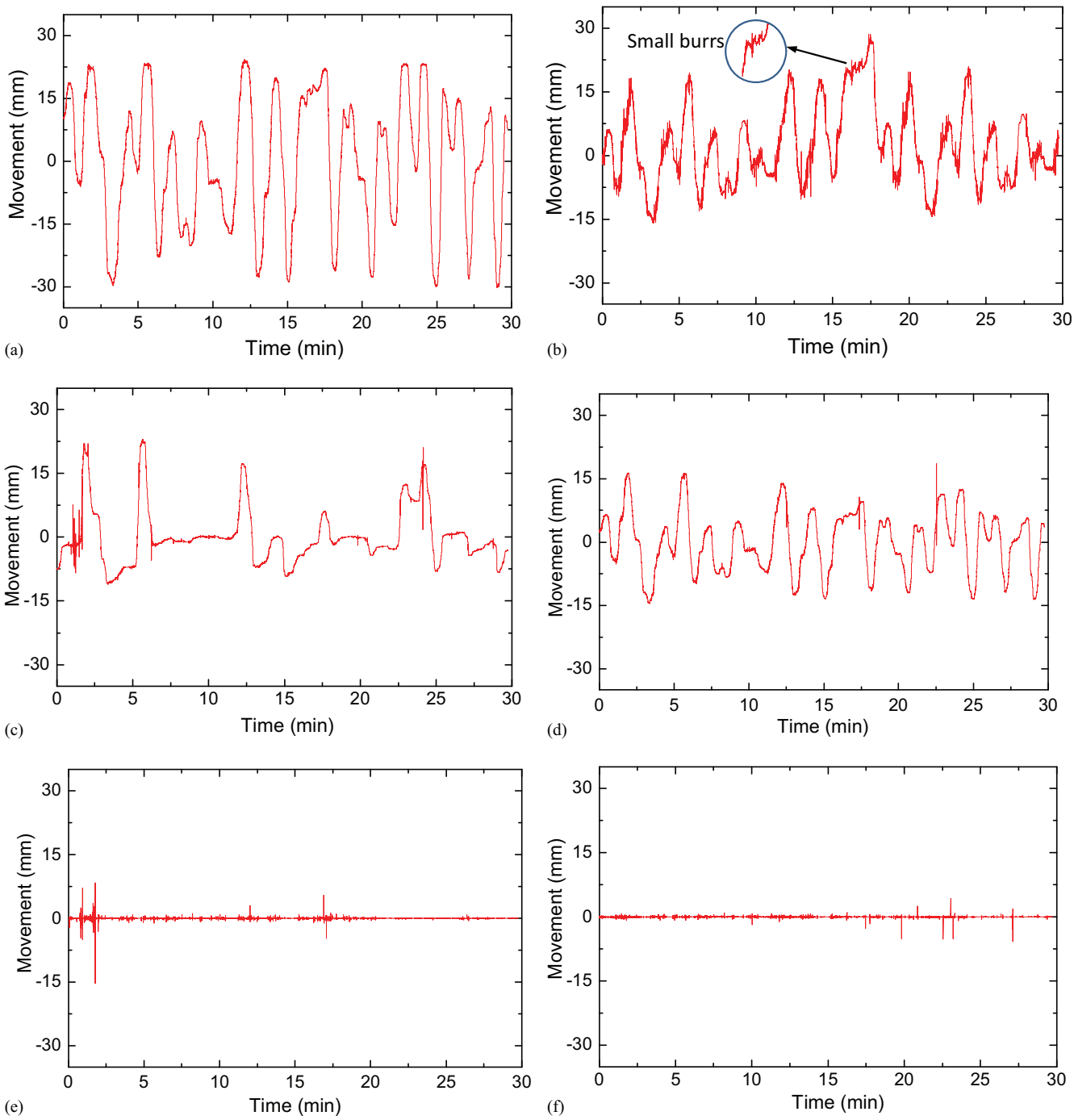

Fig. 5. Individual movement time histories of various measure points: (a) P1; (b) P2; (c) P3; (d) P4; (e) P5; (f) P6

springs at each lamella increases steadily, whereas for a single spring in δ_{27}, the maximum stress becomes 0.36 MPa.

Dynamic Analysis of Movements in Expansion Joints

Similar to the static analysis, the dynamic girder movements (obtained from measure point P7) were applied on the lamella L_0 as the input, and transient dynamic analysis (Guo et al. 2012) was conducted. As shown in Fig. 9, the relative sliding time histories of L_{25} and L_{26} were calculated and compared with the measured girder movements, in which the three time histories were synchronous, whereas the peak values of L_{25} and L_{26} were slightly smaller than those of the girder.

Fig. 9(b) shows the cumulative sliding distances of various lamellae, in which they increase significantly from L_0 to L_{26}. Taking L_{26}, for example, the cumulative sliding distance reaches 3.07 m/h, which is 68.69% of the cumulative girder movement, indicating that movements of springs near L_{26} are the majority of the total girder movements. For lamellae away from the fixed end, there is basically no relative sliding; for example, the total sliding distances are all within 50 mm for L_1–L_{14}. Such nonuniform relative sliding distances result in different types of wear of the friction material. If a cumulative distance of 20 km is taken as the design reference (CEN 2004), then the lives of the friction material of each lamellas are calculated [Fig. 9(b)], in which the friction material of L26 will be

worn after only one year of use, and rapid increase in friction coefficient could occur thereafter.

Using the rainflow counting on the calculated stress time histories, the shear stress ranges and the corresponding number of cycles of control springs are obtained (as tabulated in Table 1), in which there are 12 stress cycles greater than 0.2 MPa in springs at δ_{27} within 1 h, and the largest stress range is 0.38 MPa. Stress ranges of other springs are all less than 0.2 MPa. Based on the dynamic analysis and rainflow counting, the fatigue lives of control springs can be predicted if the *S-N* curves of these springs is available.

Theoretical Analysis of Nonuniform Movements of Lamellae

To investigate the influencing factors of the nonuniform lamella movements, a theoretical analysis is conducted as follows. Taking the nth lamella, for example, let k_1 and k_2 be the ith upper and lower sliding springs, respectively, and Δx be the precompression applied through stirrups, the precompressive force on the sliding springs can be obtained as

$$P_i = \frac{k_1 k_2}{k_1 + k_2} \Delta x_i \tag{1}$$

The sliding friction force on the lamella is

$$f_n = 2 \sum \mu P_i \tag{2}$$

where μ is the friction coefficient.

The horizontal force equivalent function of this lamella is

$$a_n k_0 \Delta\delta_n + a_{n+1} k_0 \Delta\delta_{n+1} + f_n = 0 \tag{3}$$

where a_n and a_{n+1} = number of springs in the nth and $(n+1)$th spacing, respectively; k_0 = shear stiffness of the spring; and $\Delta\delta_n$ and $\Delta\delta_{n+1}$ = change in the nth and $(n+1)$th spacing, respectively.

When the pth lamella is at the imminent moving condition, namely $\Delta\delta_p = 0$, there is

$$\begin{aligned} \Delta\delta_{p+1} &= f_n/(a_{p+1}k_0) \\ \Delta\delta_{p+2} &= 2f_n/(a_{p+2}k_0) \\ &\vdots \\ \Delta\delta_{q_{\max}} &= (q_{\max} - p)f_n/(a_{q_{\max}}k_0) \end{aligned} \tag{4}$$

where $q_{\max}$ is the serial number of the lamella at the fixed end of the expansion joint.

According to Eq. (4), due to the existence of friction forces, the change in lamella spacing becomes larger as the lamella comes closer to the fixed end of the expansion joint.

Let A_δ be the difference in the changes of two spacings, namely $A_\delta = \Delta\delta_a - \Delta\delta_b$, and A_{δ_n} can be calculated as

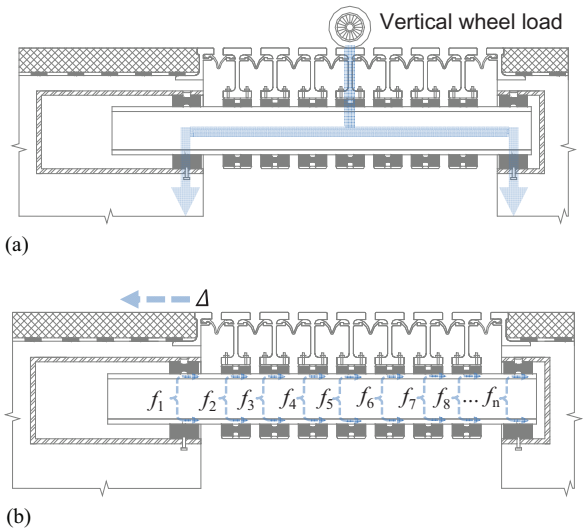

Fig. 6. (a) Vertical load and (b) horizontal load transfer paths

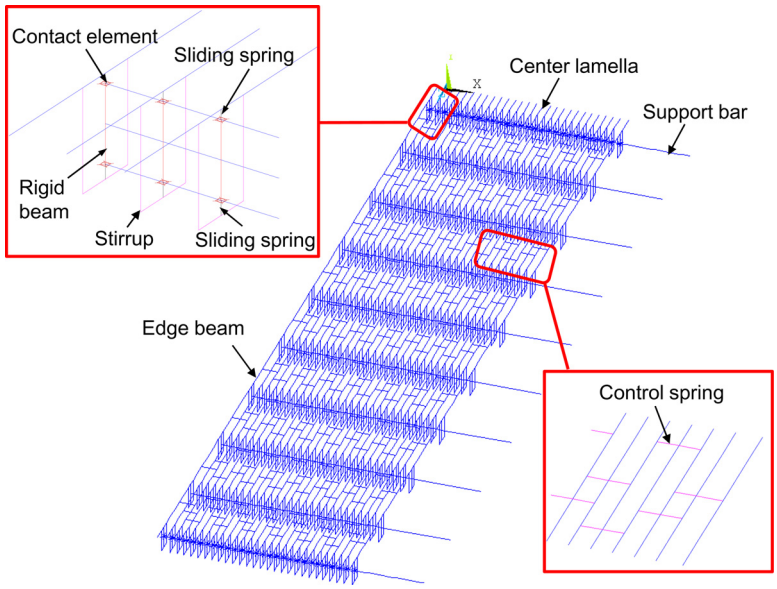

Fig. 7. FE modeling of the expansion joint

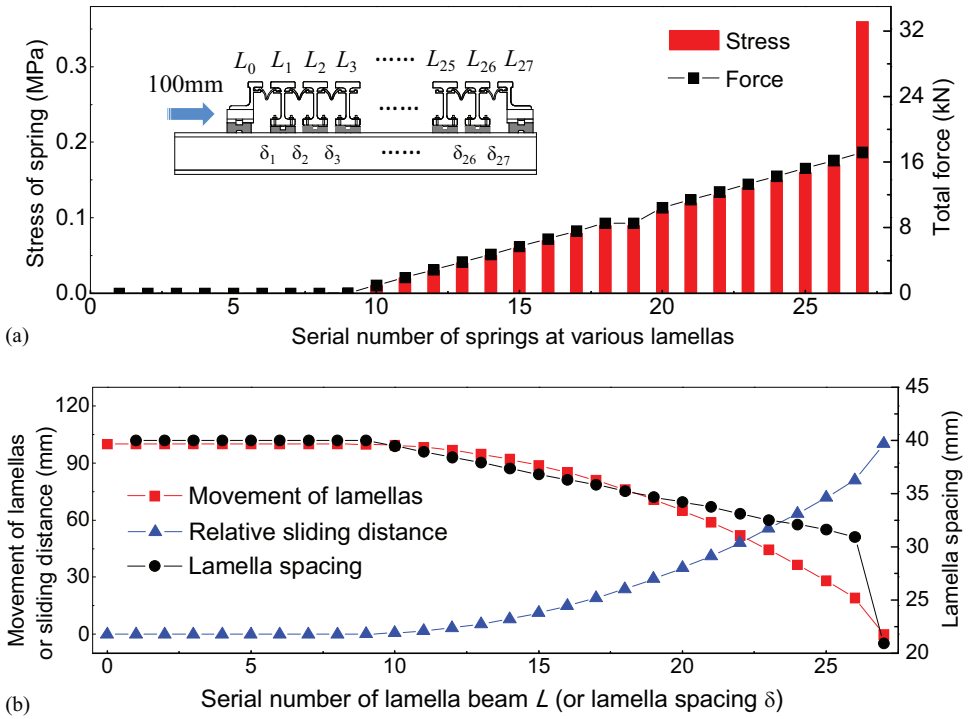

Fig. 8. Movements of lamellae and shear stresses/total forces of control springs under the static girder movement: (a) shear stresses/total forces of control springs; (b) movements, relative sliding distances of lamellae, and lamella spacing

$$A_{\delta_n} = 2\sum_{i=1}^{a_n} \mu \frac{k_1 k_2}{k_1 + k_2} \Delta x_i / (a_n k_0) \tag{5}$$

where A_{δ_n} is the proportion to friction coefficient and precompression force, and it is inversely proportional to the shear stiffness of the spring. Therefore, it is important to use the proper friction coefficient, precompression force, and shear stiffness of springs in the design to obtain the desirable behavior of the joint. In addition to the vehicle-induced girder movements, thermal-, typhoon-, and earthquake-induced movements should also be considered when determining the optimal values of these influencing factors.

Laboratory Tests on Control Springs

Because the control springs are among the most vulnerable components in expansion joints, four control springs were taken from the manufacturer for laboratory tests. The springs are made of high-quality rubber with two hemispheric metal heads with inner screw threads for connection, as shown in Fig. 10, in which a specific test system was developed to apply the shear displacements on the springs. The specimen was connected to two steel angles, and one angle was fixed to the steel base and the other angle moved synchronously with the cylinder bar and the hydraulic actuator. The cylinder bar was put in the steel tube so that it could only move along the tube.

First, the monotonic shear loading was applied, and considering that there were constraint belts used on the bridge, which only allow the maximum relative movement of 80 mm, the largest shear displacement in this test was 80 mm. As shown in Fig. 11(a), the control spring deformed gradually into an S shape, as the displacement increased. The displacement was kept for 5 min, and after the displacement was removed the spring recovered its original shape without any damage. Thereafter, four springs were tested under cyclic loading with the input target displacements of ±10, ±20, ±25, and ±30 mm, respectively, as shown in Table 2. For Specimen 1 (Test 1), there was no significant damage after 2,100,000 displacement cycles, indicating that the spring may have a long life subject to small displacements (i.e., 10 mm). The mean stiffness of Specimen 1, obtained according to the feedback actuator forces, became stable (being approximately 115.25 N/mm) after about 100,000 cycles. For Specimen 2, the failure (i.e., Pattern I) was similar to that observed on the bridge, in which there was damage at the joint of the rubber and metal head, as shown in Fig. 11(b). The test was completely terminated after the metal head fell off after 981,000 cycles, followed by a significant reduction in spring stiffness, as shown in Fig. 12 (with the mean stiffness dropping from 87.83 N/mm to below 10 N/mm). For Specimen 3, the second damage pattern was observed (i.e., Pattern II), in which cross cracks were observed after 980,000 cycles and gradually propagated, as shown in Fig. 11(c). This damage might be due to the initial material drawbacks in rubber. Generally, the crack propagation was not significant and the stiffness of this specimen basically was kept around 89.47 N/mm; therefore, the test was terminated after 1,200,000 cycles. When the displacement range became ±30 mm for Specimen 4, the spring failed only after 86,000 cycles. Again, Pattern I damage was observed with the metal head falling off and the stiffness dropping below 10 N/mm, as shown in Fig. 11(d). The stiffness in Test 1 was higher than the other tests, which might be due to the friction in the test system (i.e., friction between cylinder bar and steel tube). When the displacement ranges became larger in Tests 2–4, there were larger shear forces and the friction became relatively small.

In Tests 2 and 4, the metal head of the control spring fell off along the metal-rubber interface, which was similar to the damage observed on the RSB. This was mainly due to the different elastic modules of metal head and rubber, which concentrated the stress along the metal-rubber interface. As a result, fatigue cracking occurred along the metal-rubber interface, although the interface

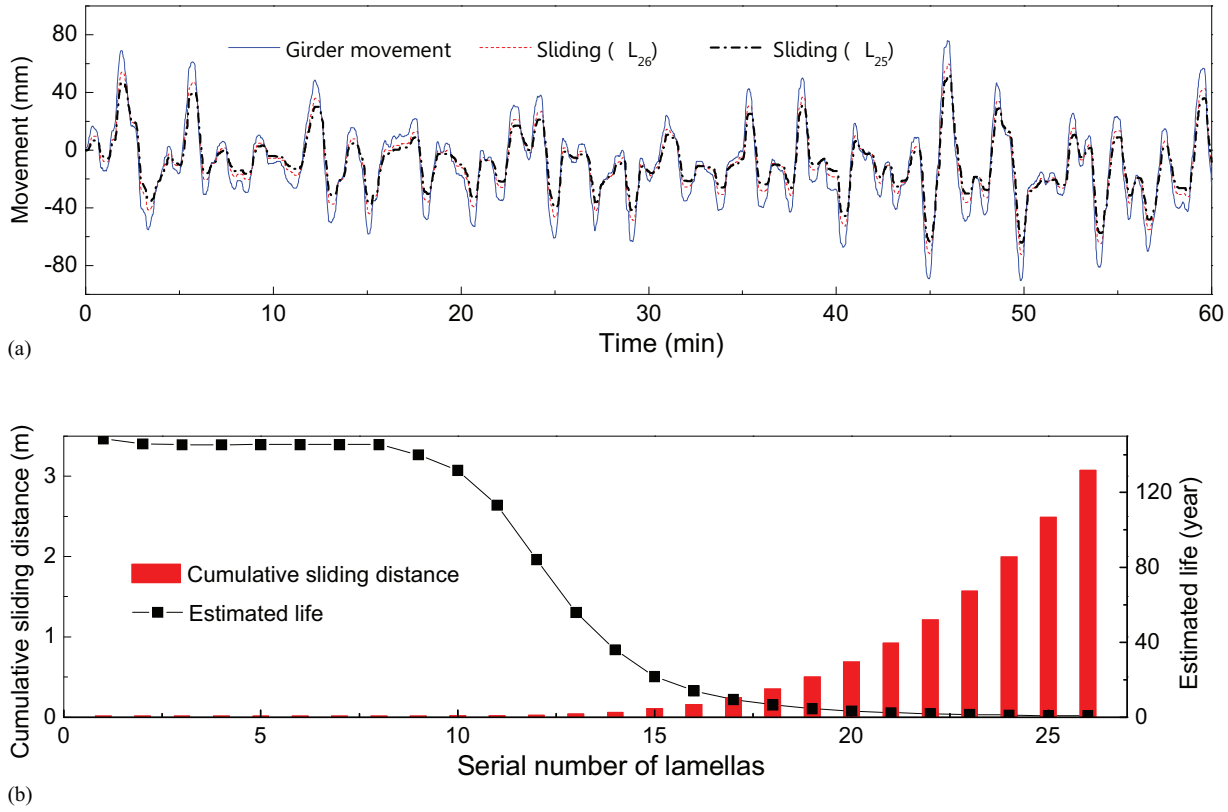

Fig. 9. Movements of lamellae under dynamic girder-end movements: (a) movement time histories; (b) cumulative sliding distances of lamellae

Table 1. Number of Cycles at Various Stress Ranges

	Stress ranges (MPa)							
Position of spring	0–0.01	0.01–0.05	0.05–0.1	0.1–0.15	0.15–0.2	0.2–0.25	0.25–0.3	≥0.3
δ_{27}	473	12	5.5	10.5	5	8	2	2
δ_{26}	491	12.5	16	10.5	2	—	—	—
δ_{25}	632	12	16	7.5	0.5	—	—	—
δ_{24}	763	16	15	5	—	—	—	—
δ_{23}	848	15	16	3	—	—	—	—
δ_{22}	922.5	12.5	14	2	—	—	—	—
δ_{21}	1,017	13	9.5	1.5	—	—	—	—
δ_{20}	1,062	13	8	—	—	—	—	—

was designed with a half-ellipsoid shape to mitigate the stress concentration. According to the test results of the four specimens, it can be concluded that as the displacement ranges increased, the life of the springs decreased significantly; therefore, the shear displacements should be properly controlled to obtain satisfactory life of the springs.

Conclusions

The modulus expansion joint is a dual-load transferring system with complicated configuration, and when used in long-span bridges, its damage mechanism is not been fully revealed. In this study, the individual movements of lamellae at different locations of the expansion joint were measured, and a FE model was developed for static and dynamic analyses. Laboratory tests on control springs were further conducted to investigate the lives of springs under various cyclic shear displacements. According to the presented study, the following conclusions can be drawn:

1. There was more damage in control springs near the edge lamella at the approximately fixed end of the expansion joint than in those underneath the center lamellae. Field measurements showed that the movements in the damaged springs were also larger than the others. Although such movements were not large in amplitude, the rapid movements resulted in considerable cumulative travel distance. Note that the accelerated wear of friction material and damage in control springs and stirrups may result in a working condition of a bridge that is different from the original design.
2. A FE model was developed in which the behaviors of vertical load bearing, horizontal sliding, and self-equivalence of lamella spacing were simulated. According to the static and

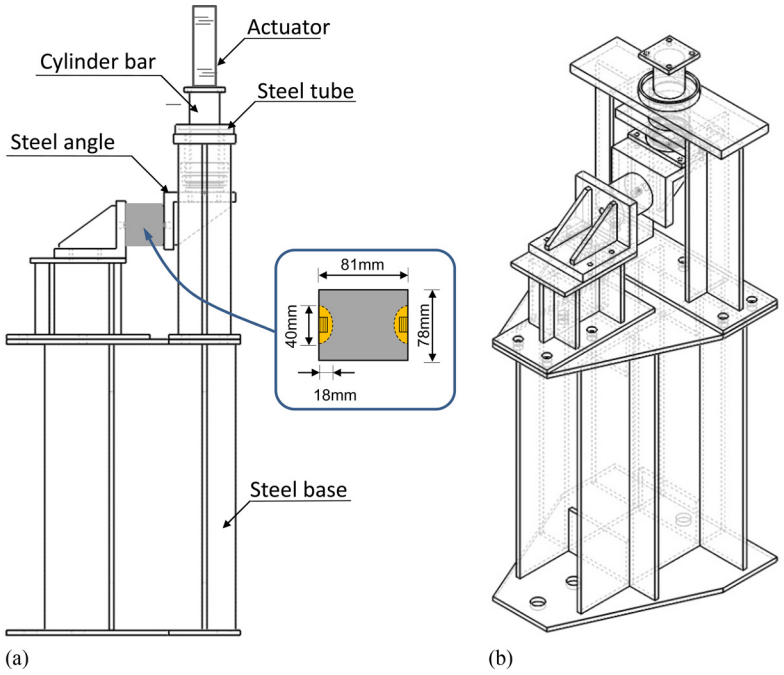

Fig. 10. Shear test system for control springs: (a) profile; (b) three-dimensional view

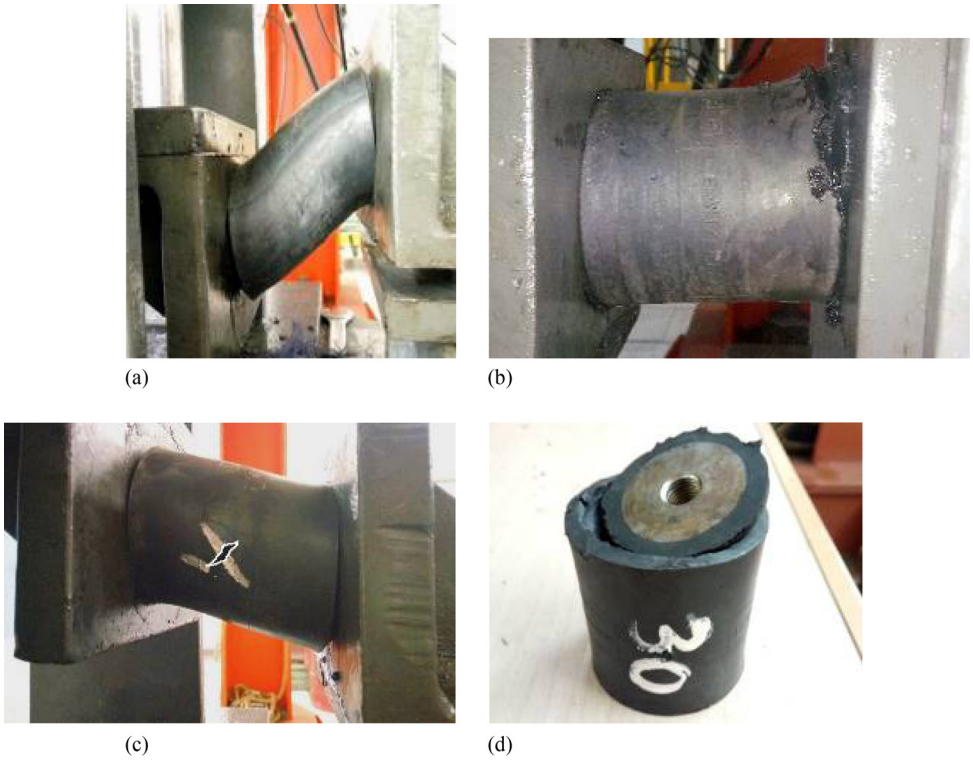

Fig. 11. Deformation of springs and damage patterns: (a) deformation under the input static displacement of 80 mm; (b) damage at the edge of the rubber; (c) cross cracks in rubber; (d) falling off of the metallic head

dynamic analyses, when there is a girder-end movement, the spacing between lamellae is nonuniform due to the friction of the sliding springs, and the springs near the edge lamella adjacent to the PSC box-girder (the almost fixed end) show more damage, which is consistent with the damage pattern observed on the bridge. Theoretical analysis further shows that the difference in the changes of two spacings is proportional to the friction coefficient and precompression and is inversely proportional to the shear stiffness of the spring.

3. A static shear test on the control spring showed that the spring can be damage free under a static shear displacement

Table 2. Cyclic Test Parameters and Results

Test	Input displacement (mm)	Damage pattern	Number of cycles ($\times 10^4$)		Mean stiffness of spring (N/mm)	
			Damage occurred	Test terminated	Prior to damage	Final
1	±10	No damage	—	210	115.25	115.25
2	±20	I	98.1	114	87.83	<10.00
3	±25	II	98.0	120	89.47	89.47
4	±30	I	8.6	15	92.07	<10.00

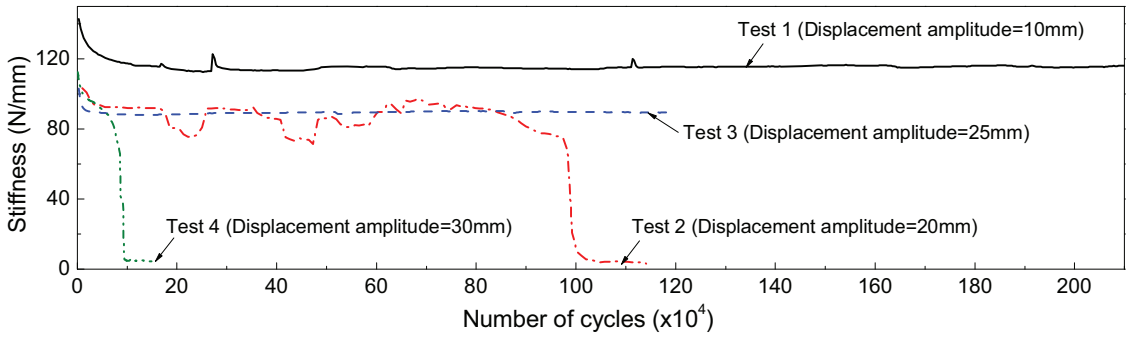

Fig. 12. Changes in spring stiffness during the tests

of 80 mm; therefore, the field-observed damage is not likely strength related. Under the cyclic loading, the life of the springs decreased significantly as the displacement amplitudes increased. Two damage patterns were observed, and the first one was the same as that observed on the bridge, whereas the second pattern showed cross cracks in the middle of the rubber cylinder. Because of the considerable costs of high-cycle tests, only four springs were tested. More test results in a future study could be beneficial to this investigation.

4. Note that cracking in the middle of the rubber cylinder (i.e., damage Pattern II) did not result in a significant loss of stiffness; therefore, the shape of the control spring might be optimized by using a slightly reduced cross section in the middle of the rubber cylinder. Also, according to the FE and theoretical analyses, more control springs should be used near the edge lamellae adjacent to the PSC box-girders, although the original design was the opposite, and larger precompression forces may also be used in springs at this region. In addition, because the damage of the control springs was essentially due to the fast girder movements, it could be an effective measure to install velocity-dependent viscous dampers at girder ends for damage mitigation.

Acknowledgments

Support from the Natural Science Foundation of Jiangsu under Grant BK20130023 and the Education Department of Jiangsu under Grant JHB2012-1 is gratefully acknowledged.

References

AASHTO. (2012). "Section 14: Joints and bearings." *AASHTO LRFD bridge design specifications*, 6th Ed., Washington, DC, 1–89.
ANSYS. (2005). *ANSYS version10.0: User's manual*, Canonsburg, PA.
ANSYS 10 [Computer software]. ANSYS, Canonsburg, PA.
Baker Engineering and Energy. (2006). "Evaluation of various types of bridge deck joints." *Final Rep. 510*, Arizona DOT, Phoenix.
Butterworth, S. (1930). "On the theory of filter amplifiers." *Wireless Eng.*, 7(Oct), 536–541.
Cao, Y., Yim, J., Zhao, Y., and Wang, M. L. (2011). "Temperature effects on cable stayed bridge using health monitoring system: A case study." *Struct. Health Monit.*, 10(5), 523–537.
CEN (European Committee for Standardization). (2004). "Structural bearings—Part 2: Sliding elements." *BS EN1337-2*, Brussels, Belgium.
Chouw, N., and Hao, H. (2008). "Significance of SSI and nonuniform near-fault ground motions in bridge response I: Effect on response with conventional expansion joint." *Eng. Struct.*, 30(1), 141–153.
Crocetti, R., and Edlund, B. (2003). "Fatigue performance of modular bridge expansion joints." *J. Perform. Constr. Facil.*, 10.1061/(ASCE)0887-3828(2003)17:4(167), 167–176.
Dexter, R., Osberg, C., and Mutziger, M. (2001). "Design, specification, installation, and maintenance of modular bridge expansion joint systems." *J. Bridge Eng.*, 10.1061/(ASCE)1084-0702(2001)6:6(529), 529–538.
Ding, Y., Zhang, W., and Au, F. T. (2016). "Effect of dynamic impact at modular bridge expansion joints on bridge design." *Eng. Struct.*, 127(Nov), 645–662.
Feng, D., and Feng, M. Q. (2016). "Output-only damage detection using vehicle-induced displacement response and mode shape curvature index." *Struct. Contr. Health Monit.*, 23(8), 1088–1107.
Guo, T., Frangopol, D. M., and Chen, Y. (2012). "Fatigue reliability assessment of steel bridge details integrating weigh-in-motion data and probabilistic finite element analysis." *Comput. Struct.*, 112–113(Dec), 245–257.
Guo, T., Liu, J., and Huang, L. Y. (2016). "Investigation and control of excessive cumulative girder movements of long-span steel suspension bridges." *Eng. Struct.*, 125(Oct), 217–226.
Guo, T., Liu, J., Zhang, Y., and Pan, S. (2015). "Displacement monitoring and analysis of expansion joints of long-span steel bridges with viscous dampers." *J. Bridge Eng.*, 10.1061/(ASCE)BE.1943-5592.0000701, 04014099.
MAGEBA. (2008). "*Modular expansion joints– TENSA-MODULAR LR & LR-LS*, Shanghai, China.

McCarthy, E., Wright, T., Padgett, J., DesRoches, R., and Bradford, P. (2014). "Development of an experimentally validated analytical model for modular bridge expansion joint behavior." *J. Bridge Eng.*, 10.1061/(ASCE)BE.1943-5592.0000521, 235–244.

Roeder, C. W. (1998). "Fatigue and dynamic load measurements on modular expansion joints." *Constr. Build. Mater.*, 12(2), 143–150.

Sun, Z., and Zhang, Y. (2016). "Failure mechanism of expansion joints in a suspension bridge." *J. Bridge Eng.*, 10.1061/(ASCE)BE.1943-5592.0000942, 05016005.

Zhao, Y., and Roddis, W. K. (2000). "Fatigue crack investigation for the Arkansas River bridge in Hutchinson, Kansas." *Constr. Build. Mater.*, 14(5), 287–295.